

Kinetics of the Decomposition of 1,1,1-Trimethyldisilane and of Trimethylsilylgermane and of Relative Rates of Silylene Insertion into Silicon-Hydrogen Bonds

D. P. Paquin and M. A. Ring*

Contribution from the Department of Chemistry, San Diego State University,
San Diego, California 92182. Received July 2, 1976

Abstract: The decomposition of $(\text{CH}_3)_3\text{SiSiH}_3$ and $(\text{CH}_3)_3\text{SiGeH}_3$ was examined and found to decompose into $(\text{CH}_3)_3\text{SiH}$ and SiH_2 or GeH_2 . The Arrhenius parameters for these decompositions were: $\log k = (14.48 \pm 0.3) - (48.0 \pm 0.5)/\theta$ and $\log k = (13.56 \pm 0.3) - (34.2 \pm 0.5)/\theta$, respectively, where $\theta = (2.3)(0.001987)T$, kcal/mol. These A factors and those reported for Si_2H_6 , $\text{CH}_3\text{Si}_2\text{H}_5$, and Si_3H_8 are analyzed in terms of a H atom bridged transition state. The relative rates of SiH_2 insertion into SiH_4 vs. CH_3SiH_3 and into Si_2H_6 vs. $(\text{CH}_3)_3\text{SiH}$ were obtained as a function of temperature to obtain relative A factors and differences in activation energies. The relative A factors are related to the decomposition A factors.

The homogeneous thermal decompositions of the parent polysilanes, unlike their hydrocarbon analogues, occur via a 1,2-hydrogen atom shift forming a silylene and a silane.¹⁻³ These decompositions are the reverse of silylene insertion reactions into silicon-hydrogen bonds. Thus the decomposition Arrhenius parameters can be used to obtain information concerning the insertion reactions.

Arrhenius parameters have been obtained for the decompositions of Si_2H_6 ,⁴ $\text{CH}_3\text{Si}_2\text{H}_5$,⁵ and Si_3H_8 ⁵ and these values are listed in Table I. The higher A factors noted for reactions 2 and 4 compared to those for reactions 1, 3, and 5 were explained⁵ by an activated complex containing a bridging H atom between a tetravalent silicon (forming the silylene) and a pentavalent silicon (forming the silane). It was suggested⁵ that the pentavalent silicon atom in the activated complex has relatively weak bonds so that the vibrational frequencies associated with this center are relatively low. When a heavy group (CH_3 or SiH_3) is bound to this center the presumed lower frequencies would yield higher entropies of activation and thus higher A factors.

In this paper, we report our results on the decomposition of $(\text{CH}_3)_3\text{SiSiH}_3$ to further examine this model. We also report results on the decomposition of $(\text{CH}_3)_3\text{SiGeH}_3$ to determine the effect of replacement by germanium. It has been demonstrated that SiH_3GeH_3 decomposes by a 1,2-H atom shift⁶ to form SiH_4 and GeH_2 .

The A factors for the silylene insertion reactions can be obtained from the A factors of the decomposition reactions and calculated values of ΔS^\ddagger for the insertion reactions. We have obtained relative rates of SiH_2 insertion into SiH_4 vs. CH_3SiH_3 and Si_2H_6 vs. $(\text{CH}_3)_3\text{SiH}$ as a function of temperature to obtain relative A factors and differences in activation energies for the insertion reactions. The relative A factors are compared to the calculated ratios to obtain support for the apparently high values of the A factors for reactions 2 and 4.

Experimental Section

The decomposition kinetics were obtained in a grease-free high vacuum system described previously.⁵ Inner walls of the reaction cell were deactivated by decomposing SiH_4 at 400 °C (or GeH_4 at 300 °C) and then evacuating at this temperature for 24 h. This procedure generates a silicon mirror via breakdown of the polymeric silicon hydride formed on the surface.⁷

Reactant and product concentrations in the kinetic runs were followed quantitatively relative to an inert internal standard (C_2H_6) using gas-liquid chromatography as previously described.⁵ To avoid complications due to secondary reactions of products, the decomposition kinetics were only followed over the first 5% of reaction.

The reactants, $(\text{CH}_3)_3\text{SiSiH}_3$ and $(\text{CH}_3)_3\text{SiGeH}_3$, were obtained via coupling of KSiH_3 or KGeH_3 with $(\text{CH}_3)_3\text{SiCl}$.⁸ Preliminary studies of the decomposition of $(\text{CH}_3)_3\text{SiSiH}_3$ were carried out in a recirculating flow system consisting of a Toepler pump, thermal zone, and a cold "U"-trap which set the pressure of the reactants and trapped the less-volatile products. To avoid surface reactions on the Vycor surface, a silicon mirror was deposited via silane decomposition. In a typical experiment, 0.82 mmol of $(\text{CH}_3)_3\text{SiSiH}_3$ was pyrolyzed (at 25 mmHg) with the cold trap at -36 °C. After 3 h at 400 °C, 0.68 mmol was consumed. The products were isolated by trap to trap distillations and identified by GLC and infrared and mass spectroscopy. The fraction passing a -196 °C trap (0.04 mmol) was H_2 (96%) and CH_4 (4%). The fraction condensed at -196 °C having passed a -95 °C trap was $(\text{CH}_3)_3\text{SiH}$ (0.47 mmol). The products condensed at -63 °C were $(\text{CH}_3)_3\text{SiSi}_2\text{H}_5$ (0.2 mmol) and possibly $(\text{CH}_3)_3\text{SiSi}_3\text{H}_7$. The mass spectrum of this fraction at 15 V contained the parent ion, $(\text{CH}_3)_3\text{SiSi}_2\text{H}_5^+$, m/e 134, and $(\text{CH}_3)_3\text{Si}^+$, m/e 73, as the largest peaks. Other ions expected from $(\text{CH}_3)_3\text{SiSi}_2\text{H}_5$ were present. At 70 V, the $(\text{CH}_3)_3\text{SiSi}_3\text{H}_7^+$ ion, m/e 164, was observed. The proton NMR spectrum of $(\text{CH}_3)_3\text{SiSi}_2\text{H}_5$ in CCl_4 consisted of a singlet (CH_3 -) at δ 0.21, a quartet (SiH_2 -) at δ 2.79, and a triplet (SiH_3 -) at δ 3.13 with relative intensities 9.4 (including impurities):1.9:3.0. The $\text{SiH} = \text{SiH}'$ coupling was 3.6 Hz.

Preliminary studies of the decomposition of $(\text{CH}_3)_3\text{SiGeH}_3$ were also carried out in the recirculating flow system. In a typical experiment over a germanium surface, 0.55 mmol of $(\text{CH}_3)_3\text{SiGeH}_3$ was pyrolyzed at 260 °C. After 3 h with the cold trap at -45 °C, 0.40 mmol of reactant was consumed. The products were H_2 (0.02 mmol), CH_4 (0.001 mmol), $(\text{CH}_3)_3\text{SiH}$ (0.28 mmol), $(\text{CH}_3)_3\text{SiGe}_2\text{H}_5$ (0.1 mmol), and a trace of $(\text{CH}_3)_3\text{SiGe}_3\text{H}_7$. The mass spectrum (15 V) of the product fraction condensed at -45 °C consisted of the following ions in order of decreasing intensity: $(\text{CH}_3)_3\text{Si}^+$, $(\text{CH}_3)_3\text{SiGeH}_2^+$, $(\text{CH}_3)_3\text{SiGe}_2\text{H}_5^+$, and $(\text{CH}_3)_3\text{SiGe}_3\text{H}_7^+$. The intensity due to the last ion was very small.

The relative rates of the insertion of SiH_2 into SiH_4 vs. CH_3SiH_3 and into $(\text{CH}_3)_3\text{SiH}$ vs. Si_2H_6 were carried out in the same reaction system used to obtain the kinetics of the decompositions of $(\text{CH}_3)_3\text{SiSiH}_3$ and $(\text{CH}_3)_3\text{SiGeH}_3$. The SiH_2 was generated from $(\text{CH}_3)_3\text{SiSiH}_3$ for the SiH_4 - CH_3SiH_3 competition and from Si_2H_6 for the $(\text{CH}_3)_3\text{SiH}$ - Si_2H_6 competition.

Results

The pyrolysis of $(\text{CH}_3)_3\text{SiSiH}_3$ in a recirculating flow system containing a "U" trap cooled to -36 °C was examined over a silicon surface at 400 °C. The volatile products were $(\text{CH}_3)_3\text{SiH}$, $(\text{CH}_3)_3\text{SiSi}_2\text{H}_5$, possibly $(\text{CH}_3)_3\text{SiSi}_3\text{H}_7$, and very small quantities of H_2 . The absence of SiH_4 and small yield of H_2 suggest the decomposition did not occur via silicon-silicon rupture since the SiH_3 radicals thus formed would abstract H atoms to form SiH_4 or react in a chain sequence to

Table I. Arrhenius Parameters for the Pyrolysis of Silanes^a

$\text{Si}_2\text{H}_6 \rightarrow \text{SiH}_2 + \text{SiH}_4$	(1)
$\log k_1(\text{s}^{-1}) = 14.5 - 49.3/\theta$	
$\text{CH}_3\text{Si}_2\text{H}_5 \rightarrow \text{SiH}_2 + \text{CH}_3\text{SiH}_3$	(2)
$\log k_2(\text{s}^{-1}) = 15.28 - 50.75/\theta$	
$\text{CH}_3\text{Si}_2\text{H}_5 \rightarrow \text{CH}_3\text{SiH} + \text{SiH}_4$	(3)
$\log k_3(\text{s}^{-1}) = 14.14 - 49.89/\theta$	
$\text{Si}_3\text{H}_8 \rightarrow \text{SiH}_2 + \text{Si}_2\text{H}_6$	(4)
$\log k_4(\text{s}^{-1}) = 15.69 - 52.99/\theta$	
$\text{Si}_3\text{H}_8 \rightarrow \text{SiH}_3\text{SiH} + \text{SiH}_4$	(5)
$\log k_5(\text{s}^{-1}) = 14.68 - 49.24/\theta$	

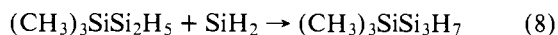
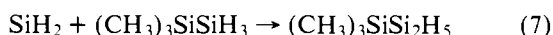
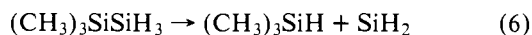
^a $\theta = (2.3)(0.001\ 987)T$, kcal/mol.

Table II. Data on the Pyrolysis of $(\text{CH}_3)_3\text{SiSiH}_3$

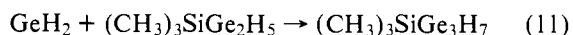
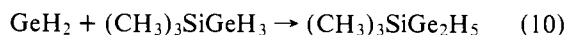
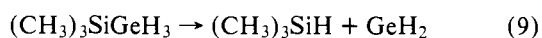
Run no.	Initial pressure of $(\text{CH}_3)_3\text{Si}_2\text{H}_3$ (mmHg)	Total pressure $\text{C}_2\text{H}_6 + (\text{CH}_3)_3\text{Si}_2\text{H}_3$ (mmHg)	Rate constants for $(\text{CH}_3)_3\text{SiH}$ formation ($\text{s}^{-1} \times 10^6$)
$\bar{T} = 530.2 \pm 0.1$ K			
1	47	50	5.03
2	16	17	4.76
3	33	35	4.85
$\bar{T} = 538.8 \pm 0.1$ K			
4	54	61	9.51
5	46	52	10.1
6	31	35	10.0
$\bar{T} = 545 \pm 2$ K			
7	117	130	23.3 ^a (16.7) ^b
8	58	64	25.3 ^a (16.7) ^b
$\bar{T} = 549.2 \pm 0.1$ K			
9	54	57	23.4
10	69	77	23.4
11	39	45	23.7
$\bar{T} = 559.5 \pm 0.1$ K			
12	31	33	52.3
13	53	56	53.2
14	32	33	52.4
15	54	57	52.7

^a Carried out in a separate vessel with a surface/volume ratio increased by a factor of 12.1. ^b Calculated from other runs.

ultimately yield H_2 . The products formed are consistent with an initial 1,2-H atom shift forming $(\text{CH}_3)_3\text{SiH}$ and SiH_2 .



In a similar fashion, the pyrolysis of $(\text{CH}_3)_3\text{SiGeH}_3$ in the same flow system over a germanium surface at 260 °C with the "U" trap cooled to -45 °C yielded $(\text{CH}_3)_3\text{SiH}$, $(\text{CH}_3)_3\text{SiGe}_2\text{H}_5$, probably $(\text{CH}_3)_3\text{SiGe}_3\text{H}_7$, and a very small quantity of H_2 . These results suggest the decomposition of $(\text{CH}_3)_3\text{SiGeH}_3$ also occurs via a 1,2-H atom shift.



The kinetics of thermal decomposition of $(\text{CH}_3)_3\text{SiSiH}_3$ was examined in the temperature range from 530 to 500 K over a silicon mirror. Similarly the $(\text{CH}_3)_3\text{SiGeH}_3$ decomposition was examined over a germanium surface in the temperature range from 389 to 406 K. Kinetic data for these decompositions

Table III. Typical Reactant and Product Pressures as a Function of Time for the Pyrolysis of $(\text{CH}_3)_3\text{SiSiH}_3$

Run no. Table II	Time (s)	Pressure (mmHg) ^a $(\text{CH}_3)_3\text{Si}_2\text{H}_3$	$(\text{CH}_3)_3\text{SiH}$
3	0	33.0	
	2687	32.7	0.412
	4883	32.1	0.716
	7180	31.4	1.18
	8893	30.8	1.33
4	0	54.0 ^b	
	1817		0.98
	3641		1.87
	5411		2.78
	7255		3.73
	8	0	58.0 ^b
13	1159		1.75
	1836		2.70
	2533		3.38
	3126		4.32
	0	53.0 ^b	
	631		1.81
	1344		4.45
	2072		6.26

^a Pressures have been adjusted to account for decrease in total pressure resulting from aliquot sampling. ^b Product pressures not required for analysis.

Table IV. Data on the Pyrolysis of $(\text{CH}_3)_3\text{SiGeH}_3$

Run no.	Initial pressure of $(\text{CH}_3)_3\text{SiGeH}_3$ (mmHg)	Total pressure $\text{C}_2\text{H}_6 + (\text{CH}_3)_3\text{SiGeH}_3$ (mmHg)	Rate constants for $(\text{CH}_3)_3\text{SiH}$ formation ($\text{s}^{-1} \times 10^6$)
$\bar{T} = 389.0 \pm 0.1$ K			
1	57	64	2.33
2	57	63	2.20
3	48	52	2.27
4	21	26	2.10
$\bar{T} = 395.9 \pm 0.1$ K			
5	40	50	4.93
6	42	50	4.99
7	35	47	5.25
$\bar{T} = 400.2 \pm 0.1$ K			
8	20	26	7.71
9	23	29	7.34
$\bar{T} = 406.3 \pm 0.1$ K			
10	29	57	14.9
11	22	45	14.9
12	17	34	15.3
$\bar{T} = 404 \pm 3$ K			
13	50	110	13.2 ^a (11.6) ^b
14	37	74	13.2 ^a (11.6) ^b
15	48	96	13.6 ^a (11.6) ^b

^a Carried out in a separate vessel with a surface/volume ratio increased by a factor of 12.1. ^b Calculated from other data.

are listed in Tables II and IV. In Tables III and V are listed experimentally determined product pressures as a function of time for a representative run at each temperature. The decomposition kinetics were found to be first order. Thus two-to-threefold variations in concentration resulted in corresponding variations in rate. The rate constants were also unaffected by two-to-threefold variations in total pressure and within experimental error, invariant to large changes in surface to volume ratios ($S/V \approx 1$ cm⁻¹ in most runs) $S/V \approx 12.1$ cm⁻¹ in runs 7 and 8, Table II, and runs 13–15, Table IV). Therefore the primary decomposition reactions (6 and 9) are homogeneous, unimolecular processes in their high pressure

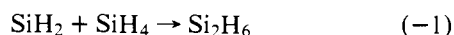
Table V. Typical Reactant and Product Pressures as a Function of Time for the Pyrolysis of (CH₃)₃SiGeH₃

Run no. Table IV	Time (s)	Pressure (mmHg) ^a	
		(CH ₃) ₃ SiGeH ₃	(CH ₃)SiH
2	0	57.0 ^b	
	2051		0.291
	3773		0.530
	5376		0.764
	7284		0.855
5	0	40 ^b	
	1311		0.278
	2450		0.522
	3853		0.726
	4909		0.953
10	0	29 ^b	
	1257		0.550
	2377		0.931
	4946		1.95
	6601		2.53
15	0	48 ^b	
	2183		1.39
	4253		2.71
	6774		4.02
	8540		5.52

^a Pressures have been adjusted to account for decrease in total pressure resulting from aliquot sampling. ^b Product pressures not required for analysis.

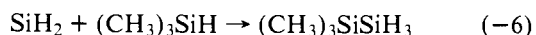
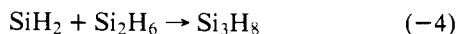
region. The Arrhenius parameters for these decompositions are listed in Table VI.

The relative rates of the reaction of SiH₂ with SiH₄ vs. CH₃SiH₃ were obtained in the static system over a silicon mirror. This study was carried out by the decomposition of (CH₃)₃SiSiH₃ (SiH₂ source) in the presence of SiH₄ and CH₃SiH₃ followed by determination of the ratio of Si₂H₆ and CH₃Si₂H₅.



Since the decomposition rate constants for Si₂H₆ and CH₃Si₂H₅ are similar at these temperatures,^{4,5} secondary decompositions will not alter the initial ratio of formation of Si₂H₆ and CH₃Si₂H₅ especially when the products are examined after a few percent of reaction. The results of these experiments are listed in Table VII.

The relative rates of the reaction of SiH₂ with Si₂H₆ vs. (CH₃)₃SiH were also examined. These experiments were carried out by the decomposition of Si₂H₆ in the presence of (CH₃)₃SiH in our kinetic apparatus. The ratio of Si₃H₈ to (CH₃)₃SiSiH₃ was obtained by gas chromatography.



The results of these experiments are listed in Table VIII.

Discussion

Activation Energies. The activation energy for the homogeneous thermal decomposition of (CH₃)₃SiSiH₃ (48 kcal/mol) is similar to those for the other polysilanes (Table I) and is much less than the predicted value of $D((\text{CH}_3)_3\text{SiSiH}_3)$ which would be about 80 kcal/mol.⁹ This result is consistent with the mechanism proposed (reactions 6–8). Similarly, the value of 34 kcal/mol for the activation energy of the decomposition of (CH₃)₃SiGeH₃ is much lower than the predicted value for $D((\text{CH}_3)_3\text{SiGeH}_3)$ which is greater than 75 kcal/mol.¹⁴ This result is also consistent with the proposed mechanism (reactions 9–11).

Table VI. Arrhenius Parameters for Trimethylsilane Formation in the Pyrolysis of 1,1,1-Trimethyldisilane and Trimethylsilylgermane

Reactant	Log <i>A</i> (s ⁻¹)	<i>E</i> (kcal/mol)
(CH ₃) ₃ SiSiH ₃	14.48 ± 0.3	48.0 ± 0.5
(CH ₃) ₃ SiGeH ₃	13.56 ± 0.3	34.2 ± 0.5

Table VII. Relative Insertion Rates of Silylene into Methylsilane vs. Silane at Several Temperatures^b

<i>T</i> (K)	(<i>k</i> ₋₂ / <i>k</i> ₋₁) _{av}
519.1	0.967 ± 0.05
529.1	1.05 ± 0.05
544.1	1.17 ± 0.08
560.0	1.30 ^a

^a Values ranged from 1.30 to 1.46. ^b Log (*A*₋₂/*A*₋₁) = 1.7 ± 0.4. *E*₋₂ - *E*₋₁ = 4.2 ± 1.2 kcal/mol.

Table VIII. Relative Insertion Rates of Silylene into Trimethylsilane vs. Disilane^a

<i>T</i> (K)	(<i>k</i> ₋₆ / <i>k</i> ₋₄)	<i>T</i> (K)	(<i>k</i> ₋₆ / <i>k</i> ₋₄)
529.3	0.57 ± 0.06	560.2	0.47 ± 0.05
	0.59 ± 0.06		0.49 ± 0.05
	0.55 ± 0.06		0.50 ± 0.05

^a Log (*A*₋₄/*A*₋₆) = 1.4 ± 0.5, *E*₋₄ - *E*₋₆ = 2.9 ± 1.5 kcal/mol.

Nature of Activated Complexes. The *A* factors for these two decompositions and those listed in Table I can be used to examine the activated complexes.

The *A* factor is related to the intrinsic entropy of activation, Δ*S*_i[‡], by eq 12

$$A = \sigma \frac{ek\bar{T}}{h} e^{\Delta S_i^\ddagger/R} \quad (12)$$

where σ is the reaction path degeneracy, *k* is the Boltzmann constant, *h* is Planck's constant, and \bar{T} is the average temperature. In Table IX, we list the values of Δ*S*_i[‡] for reactions 1–6 and 9 based on the experimental values of *A* and the appropriate reaction path degeneracies.

The intrinsic entropy of activation, Δ*S*_i[‡], can be equated to the sum of contributing factors (eq 13).

$$\Delta S_i^\ddagger = \Delta S_{iR}^\ddagger + \Delta S_{RB}^\ddagger + \Delta S_{v}^\ddagger \quad (13)$$

The contributions, Δ*S*_{iR}[‡] (from the loss of the SiH₃ or GeH₃ internal rotor), have been calculated by statistical thermodynamic methods¹⁵ assuming a ground state barrier of 1 kcal/mol.¹⁶ Molecular models of the transition states for the decompositions of (CH₃)₃SiSiH₃ and (CH₃)₃SiGeH₃ demonstrate that the methyl groups are more hindered there than in their ground states. The configuration of the CH₃ groups in these activated complexes resembles those in P(CH₃)₃. The nonzero contributions for Δ*S*_{RB}[‡] (from more hindered methyl rotors) listed in Table IX were calculated with ground state methyl rotational barriers of 1.85 kcal/mol as in (CH₃)₃SiH¹⁷ and transition state barriers of 2.6 kcal/mol as in P(CH₃)₃.¹⁷ The contributions to Δ*S*_i[‡] due to changes in vibrational entropy, Δ*S*_v[‡], were obtained by difference from eq 13. The other possible contributions to Δ*S*_i[‡] are very small or zero and have been assumed to be zero. These are changes due to external rotation, translation, and electronic effects.

The positive values obtained for the vibrational entropy of

Table IX. Summary of Transition State Entropy Change Contributions

Reaction	σ	Log A (s^{-1})	ΔS^\ddagger (eu) ^a	ΔS^\ddagger_{IR}	ΔS^\ddagger_{RB}	ΔS^\ddagger_v
(1) $Si_2H_6 \rightarrow SiH_2 + SiH_4$	18	14.5	-1.1	-6.2	0.0	5.1
(2) $CH_3Si_2H_5 \rightarrow SiH_2 + CH_3SiH_3$	9	15.3	3.9	-6.8	0.0	10.7
(3) $CH_3Si_2H_5 \rightarrow SiHCH_3 + SiH_4$	6	14.1	-0.77	-6.8	0.0	6.0
(4) $Si_3H_8 \rightarrow SiH_2 + Si_2H_6$	18	15.7	4.3	-6.9	0.0	11.2
(5) $Si_3H_8 \rightarrow SiHSiH_3 + SiH_4$	12	14.7	0.60	-6.9	0.0	7.5
(6) $(CH_3)_3SiSiH_3 \rightarrow SiH_2 + (CH_3)_3SiH$	9	14.5	0.27	-6.9	-0.7	7.9
(9) $(CH_3)_3SiGeH_3 \rightarrow GeH_2 + (CH_3)_3SiH$	9	13.6	-3.2	-6.4	-0.9	4.1

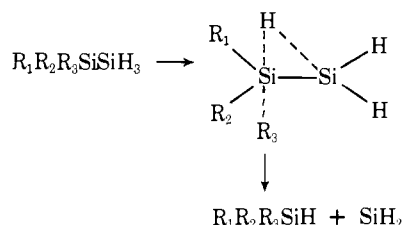
^a $\bar{T} = 545$ K for all the reactions (1-5, and 6), $\bar{T} = 398$ K for (9).

activation, ΔS^\ddagger_v , are presumed due to lower frequency vibrations associated with the pentavalent silicon center (see Figure 1), a lower frequency silicon-silicon stretch, a gain of about 1 eu due to the added torsional mode about the silicon-hydrogen-silicon three membered bridge system in the transition state, and a small decrease from the lost vibrational mode converted to the reaction path (an Si-Si-H bend).

Previously, we had suggested that the larger A factors for reactions 2 and 4 were the result of lowered frequencies for vibrational modes associated with the pentavalent silicon center. When this center is bonded to heavy groups (CH_3 or SiH_3) the lowered frequencies significantly¹⁸ raise A (via ΔS^\ddagger_v). This model would predict a very high value of ΔS^\ddagger_v (and A) for reaction 6. Our experimental value is closer to those of reactions 1, 3, and 5.

Our results imply that the order of "looseness" for the activated complexes are in the order: reactions 2, 4 > 1, 3, 5, 6 > 9. We can present a model that fits the data for reactions 1-6 and can suggest a rationalization for the lower value for reaction 9. In this model, the bond to R_3 (Scheme I) is much

Scheme I. Reaction Path of Decompositions



weaker than in the ground state while the bonds to R_1 and R_2 are slightly stronger than in the ground state.¹⁹ Thus when R_3 is a heavy group, the lowering of the frequencies would significantly¹⁸ raise ΔS^\ddagger_v . Conversely, when R_1 and R_2 are heavy, the slightly stronger bonds would decrease ΔS^\ddagger_v . Thus for reactions 1, 3, 5, and 6, where $R_1 = R_2 = R_3 = H$ or CH_3 , the values of ΔS^\ddagger_v should all be similar. That is, the heavy group "loosening" at R_3 is either absent, or compensated by heavy group "tightening" at R_1 and R_2 . For reactions 2 and 4, the model gives two different kinds of transition state geometries: $R_1 = R_2 = H$ and $R_3 = CH_3$ or SiH_3 ($\sigma/3$ paths); R_1 and $R_2 = CH_3, H$ or SiH_3, H and $R_3 = H$ ($2\sigma/3$ paths). The transition states with large groups at R_3 should be strongly entropically favored over the latter or those with $R_1 = R_2 = R_3$. Thus reactions 2 and 4 would be expected to have large positive activation entropies, mainly by the paths with heavy groups at R_3 . This is consistent with the higher A factors observed for reactions 2 and 4.

The lower intrinsic entropy (and value of ΔS^\ddagger_v) for reaction 9 indicates that its activated complex is "tighter" than those of reactions 1-6. This is consistent with its significantly lower activation energy for this reaction (i.e., less distortion of the bonds is needed to reach the transition state, hence smaller entropy effects).

Table X. Calculated Values of Log A ($atm^{-1} s^{-1}$) Insertion

Reaction (545 K)	Log A
(-1) $SiH_2 + SiH_4 \rightarrow Si_2H_6$	9.5 ^a
(-2) $SiH_2 + CH_3SiH_3 \rightarrow CH_3Si_2H_5$	10.7 ^b
(-4) $SiH_2 + Si_2H_6 \rightarrow Si_3H_8$	11.0 ^b
(-6) $SiH_2 + (CH_3)_3SiH \rightarrow (CH_3)_3SiSiH_3$	9.2 ^c

^a From $A_{1,2}$ -shift of ref 4 and S° values in ref 5. ^b From ref 5. ^c The calculated value S°_{545} for $(CH_3)_3SiSiH_3$ was 120.8 eu^{15,20} which gave a value of -33.8 eu for ΔS° insertion reaction.

Insertion Reactions—A Factors and Activation Energies. The A factors for SiH_2 insertion into the silicon-hydrogen bonds of SiH_4 , CH_3SiH_3 , Si_2H_6 , and $(CH_3)_3SiH$ can be calculated by eq 14.

$\log A$ ($atm^{-1} s^{-1}$) insertion =

$$\log A(s^{-1})_{1,2-H \text{ shift}} + \frac{\Delta S^\circ}{2.3R} (\text{insertion}) \quad (14)$$

The values calculated by eq 14 are listed in Table X. The error limits for $\log A$ (insertion) are at least ± 0.5 (0.2 from $\log A_{\text{shift}}$ and 0.3 due to the uncertainty in ΔS° (insertion)).

We obtained a value of 1.7 ± 0.4 for $\log(A_{-2}/A_{-1})$ which is within experimental error of the calculated value (1.2) from Table X. This result is consistent with the high A factor observed for reaction 2 compared to reaction 1. Cox and Purnell²⁴ obtained values of 0.34 and 0.83 for $\log(A_{-4}/A_{-2})$ and $\log(A_{-4}/A_{-6})$, respectively. The first of these values is in very good agreement with those values listed in Table X. The value obtained for $\log(A_{-4}/A_{-6})$ in this study was 1.4 ± 0.5 , while the calculated value in Table X is 1.8. For these reactions, the data at least agree that A_{-4} is significantly greater than A_{-6} .

John and Purnell²⁵ also obtained a value of -0.16 for $\log(A_{-4}/A_{-1})$. The value obtained from Table X is 1.5. However, in their experiments the Si_2H_6 , formed from the SiH_2 insertion into SiH_4 , was essentially measured by difference and thus subject to larger uncertainties.

John and Purnell²⁵ obtained a value for the activation energy for SiH_2 insertion into SiH_4 of 1.3 ± 1.1 kcal/mol. This value was *not* obtained from a straightforward plot of rate vs. $1/T$. We have found that the difference between the activation energies of SiH_2 insertion into CH_3SiH_3 vs. SiH_4 ($E_{-2} - E_{-1}$) was 4.2 ± 1.2 kcal/mol while the difference for SiH_2 insertion into Si_2H_6 vs. $(CH_3)_3SiH$ ($E_{-4} - E_{-6}$) was 2.9 ± 1.5 kcal/mol.

Additional support for significant differences in SiH_2 activation energies comes from an earlier study in this laboratory of relative insertion rates of SiH_2 into $ClSiH_3$ and Si_2H_6 .³ We found that SiH_2 insertion into $ClSiH_3$ was not observably competitive with insertion into Si_2H_6 under conditions where $ClSi_2H_5$ was as stable as Si_3H_8 .^{3,26} Thus the relative rate of SiH_2 insertion into Si_2H_6 is at least 10^2 times greater than for

ClSiH_3 in the temperature range 330–370 °C. With similar A factors, this result implies that insertion into ClSiH_3 had an activation energy at least 5 kcal/mol greater. If the A factor for insertion into Si_2H_6 were ten times higher, the difference in insertion activation energies would still have to be equal or greater than 2.5 kcal/mol. We have also observed that SiH_2 insertion into CH_3PH_2 does not compete with insertion into Si_2H_6 ³ under conditions where SiH_3PH_2 ³ was of similar stability to Si_3H_8 . Thus, again assuming similar activation entropies, the activation energy for SiH_2 insertion into CH_3PH_2 is significantly greater than for SiH_2 insertion into CH_3SiH_3 . The fact that the activation energies of SiH_2 insertion into silicon–hydrogen (and phosphorus–hydrogen) bonds can differ by as much as 3–5 kcal/mol strongly suggests that the absolute E values for all of these SiH_2 insertion reactions are significantly greater than the very low values (from 0 to 1.3 kcal/mol) previously suggested.^{4,24}

Acknowledgment. The authors are indebted to H. E. O'Neal for most valued discussions.

References and Notes

- (1) P. Estacio, M. D. Sefcik, E. K. Chan, and M. A. Ring, *Inorg. Chem.*, **9**, 1068 (1970).
- (2) M. Bowery and J. H. Purnell, *J. Am. Chem. Soc.*, **92**, 2594 (1970).
- (3) M. D. Sefcik and M. A. Ring, *J. Am. Chem. Soc.*, **95**, 5168 (1973).
- (4) M. Bowery and J. H. Purnell, *Proc. R. Soc. London, Sect. A*, **321**, 341 (1971).
- (5) A. J. Vanderwielen, M. A. Ring, and H. E. O'Neal, *J. Am. Chem. Soc.*, **97**, 993 (1975).
- (6) L. E. Elliot, P. Estacio, and M. A. Ring, *Inorg. Chem.*, **12**, 2193 (1973).
- (7) J. H. Purnell and R. Walsh, *Proc. R. Soc. London, Sect. A*, **293**, 543 (1966).
- (8) E. Amberger and E. Muhlofer, *J. Organomet. Chem.*, **12**, 55 (1968).
- (9) The reported values of $D(\text{H}_3\text{Si}-\text{SiH}_3)$ are 81¹⁰ and 84¹¹ kcal/mol while those for $D(\text{CH}_3)_3\text{Si}-\text{Si}(\text{CH}_3)_3$ are 81¹² and 80.6¹³ kcal/mol.
- (10) W. C. Steele and F. G. A. Stone, *J. Am. Chem. Soc.*, **86**, 3174 (1964).
- (11) F. E. Saalfeld and H. J. Svec, *J. Phys. Chem.*, **70**, 1753 (1966).
- (12) G. C. Hess, F. W. Lampe, and L. H. Sommer, *J. Am. Chem. Soc.*, **86**, 3174 (1964).
- (13) I. M. T. Davidson and A. V. Howard, *J. Chem. Soc., Faraday Trans. 1*, **71**, 69 (1975).
- (14) The value of $D(\text{GeH}_3-\text{SiH}_3)$ has been reported to be 99 kcal/mol.¹¹
- (15) G. N. Lewis and M. Randall, "Thermodynamics", McGraw-Hill, New York, N.Y., 1971, Chapter 27.
- (16) The silyl barrier in FSi_2H_5 is 1 kcal/mol.¹⁷
- (17) J. E. Wollrob, "Rotational Spectra and Molecular Structure", Academic Press, New York, N.Y., 1967.
- (18) Relatively small changes in frequency will only significantly change the vibrational entropy when the original vibrational frequency is below about 800 cm^{-1} and the changes become much more important as the ground state frequency decreases.
- (19) In the trigonal bipyramidal configuration the axial bonds are longer than the equatorial bonds.
- (20) The vibrational frequency estimates for the S^0_{545} calculation were based on the spectra of $(\text{CH}_3)_3\text{SiH}_3$ ²¹ and Si_3H_8 .²² The value for S^0_{545} of $(\text{CH}_3)_3\text{SiH}$ (99.8 eu) was obtained from ref 23.
- (21) D. F. Ball, P. L. Goggin, D. C. McKean, and L. A. Woodward, *Spectrochim. Acta*, **16**, 1358 (1960).
- (22) F. Feher and H. Fischer, *Naturwissenschaften*, **51**, 461 (1964).
- (23) S. W. Benson, "Thermochemical Kinetics", Wiley, New York, N.Y., 1968, p 192.
- (24) B. Cox and J. H. Purnell, *J. Chem. Soc., Faraday Trans. 1*, 859 (1975).
- (25) P. John and J. H. Purnell, *J. Chem. Soc., Faraday Trans. 1*, 1455 (1975).
- (26) R. L. Jenkins, A. J. Vanderwielen, S. P. Ruis, S. R. Gird, and M. A. Ring, *Inorg. Chem.*, **12**, 2968 (1973).

Metal–Silicon Bonded Compounds. 9.¹ The Synthesis and Structure of Bis(trimethylsilyl)magnesium 1,2-Dimethoxyethane Adduct

Alice R. Claggett, William H. Ilsley, Thomas J. Anderson, Milton D. Glick, and John P. Oliver*

Contribution from the Department of Chemistry, Wayne State University, Detroit, Michigan 48202. Received August 16, 1976

Abstract: Bis(trimethylsilyl)magnesium (I) was prepared by direct reaction of magnesium metal with bis(trimethylsilyl)mercury in either DME or THF solvent. Both chemical analyses and NMR spectral studies showed that the crystalline product obtained was the ether adduct of I. Limited variable temperature NMR studies indicate a complex reaction path is followed with formation of several silylmercury complexes. The structure of I has been determined from single-crystal x-ray data collected by counter methods. It crystallizes in the orthorhombic space group *Pbcn* with unit cell parameters $a = 16.461$ (2), $b = 9.348$ (1), and $c = 11.950$ (2) Å with four molecules of $\text{Mg}(\text{SiMe}_3)_2\text{-DME}$ per unit cell. Full-matrix least-squares refinement with fixed contributions for the hydrogen atoms gave discrepancy factors of $R_1 = 0.047$ and $R_2 = 0.054$ for 640 reflections with $I > 2.5\sigma(I)$. The magnesium atom is surrounded by two silicon atoms and two oxygen atoms which form a distorted tetrahedron. The Mg–Si distances are 2.630 (2) Å with an Si–Mg–Si angle of 125.2 (1)°, while the Mg–O distances are 2.124 (4) Å with an O–Mg–O angle of 76.3 (2)° determined by the configuration of the DME chelate ring. The dihedral angle between the Si–Mg–Si and O–Mg–O planes is 89.7°.

A number of silyl–main group metal derivatives have been reported² and in the past few years several structures have appeared which show direct silicon–metal bonds.^{3–5} These include recent examples which have silicon–mercury bonds^{4,5} and electron deficient silicon bridge bonds in silyllithium hexamer.³ Reports have appeared over the years which indicate formation of silylmagnesium species,² but no conclusive work has appeared with regard to the composition or nature of these nor have they been isolated. We now wish to report the synthesis, a few properties, and the solid state crystal and molecular structure of the first example of a compound containing

a silicon-to-magnesium bond, bis(trimethylsilyl)magnesium 1,2-dimethoxyethane.

Experimental Section

All studies were carried out using standard Schlenk tube, drybox, or high vacuum techniques. All solvents used were of standard reagent quality and were dried by refluxing over NaK or LiAlH_4 and distilled for immediate use or storage on the vacuum system. The magnesium used in the initial experiments was of high purity obtained from Dow Chemical Co.; however, subsequent studies were carried out with equal success using Grignard quality magnesium turnings. The trimethyl-